Konversi Energi dan Manufaktur

P-ISSN : 2339-2029
E-ISSN : 2622-5565

Jurnal Konversi Energi dan Manufaktur
Volume 11 Number 1 – January 2026 Page 1-8
Website : http://journal.unj.ac.id/unj/index.php/jkem
DOI: https://doi.org/10.21009/JKEM.11.1.1

Effect of SMAW Process Parameters on Hardness, Temperature Distribution, and Micro–Macro Structure of A36 Steel Welded Joints

Desrilia Nursyifaulkhair[1], Priyambodo Nur Ardi Nugroho[1*], Dianita Wardani[2], Kharismajid[1], Mochammad Karim Al Amin[1], Muhamad Eko Nur Khazi[1]

[1] *Ship Building Engineering, Politeknik Perkapalan Negeri Surabaya, East Java, 60111, Indonesia.*
[2] *Marine Engineering, Politeknik Perkapalan Negeri Surabaya, East Java, 60111, Indonesia.*
* Corresponding Author. E-mail : priyambodo@ppns.ac.id

Article information - : Received : 03-10-2025; Revised : 15-11-2025; Accepted : 24-11-2025

Abstract

The outer shell of an ISO tank plays a critical role in maintaining the integrity of its contents by withstanding temperature fluctuations, pressure, and radiation. Research on the fabrication of liquefied natural gas (LNG) tank outer shells therefore provides both scientific and practical value, particularly in ensuring mechanical reliability and structural performance. This study investigates the welding of American Society for Testing Materials (ASTM) A36 steel plates using shielded metal arc welding (SMAW) and evaluates the effect of welding parameters on mechanical and microstructural properties. Four specimens were prepared by varying welding current at 70 and 80 A on plate thicknesses of 4 and 12 mm. The results indicate that both current and thickness significantly influence the weld zone microstructure, with transformations from ferrite–pearlite in the base metal to widmanstätten and acicular ferrite in the weld metal. In terms of mechanical performance, the highest hardness value of 198.387 HVN was recorded in the 4 mm specimen welded at 70 A, demonstrating the strong dependence of hardness on combined current and thickness conditions. These findings contribute to optimizing welding parameters for the safe and reliable application of LNG tank outer shells.

Keywords: SMAW; A36 steel; hardness; temperature distribution; micro-macrostructure.

1. Introduction

The outer shell of International Organization for Standard (ISO) tanks serves as a primary barrier to protect liquefied natural gas (LNG) from environmental factors such as temperature fluctuations, external pressure, and radiation that could compromise safety and product integrity [1], [2]. The fabrication of ISO tank shells requires materials with adequate mechanical strength and microstructural stability to withstand operational stresses during storage and transport, particularly with ship [3]. American Society for Testing Materials (ASTM) A36 steel is often selected for such applications due to its favorable combination of weldability [4], availability, and cost-effectiveness [5]. However, welding-induced changes in microstructure and mechanical properties remain critical challenges in ensuring structural performance and long-term reliability [6].

Extensive studies have demonstrated that welding parameters, particularly current and plate thickness, significantly influence the quality of weld joints [7]. Previous research [8] emphasized that welding current governs arc energy and heat input, thereby affecting bead geometry, hardness, and microstructural evolution. Similarly, researchers highlighted that plate thickness influences heat dissipation, residual stress, and distortion [9] during welding [10]. Investigations on ASTM A36 steel also reported that variations in welding heat input can cause transformations in the weld zone [11], including the formation of ferrite, pearlite, widmanstätten structures, and acicular ferrite, each with distinct mechanical implications [12].

Despite these findings, most studies have focused on general applications of structural steel or thick-plate welding, with limited emphasis on medium- to thin-plate configurations relevant to LNG tank fabrication [13]. Furthermore, systematic evaluation of current and thickness combined effects on hardness and microstructure in shielded metal arc welding (SMAW)-welded ASTM A36 remains sparse.

Konversi Energi dan Manufaktur
P-ISSN : 2339-2029
E-ISSN : 2622-5565
Jurnal Konversi Energi dan Manufaktur
Volume 11 Number 1 – January 2026 Page 1-8
Website : http://journal.unj.ac.id/unj/index.php/jkem
DOI: https://doi.org/10.21009/JKEM.11.1.1

Therefore, this research investigates the influence of welding current (70 A and 80 A) and plate thickness (4 mm and 12 mm) on the microstructure and hardness of ASTM A36 steel welds. The novelty of this work lies in its direct application to ISO tank outer shells, providing insights into optimal welding conditions for balancing mechanical properties and microstructural stability. The purpose of this study is to identify parameter combinations that enhance weld quality, ensuring safety and durability in LNG tank applications.

2. Experimental Methods

2.1. Materials and Specimens

The base material used in this research was ASTM A36 structural steel, commonly applied in ISO tank fabrication. Two plate thicknesses, 4 and 12 mm, were prepared with dimensions of 150 × 100 mm. The chemical composition was confirmed to comply with ASTM A36, and the joint design is shown in Figure 1.

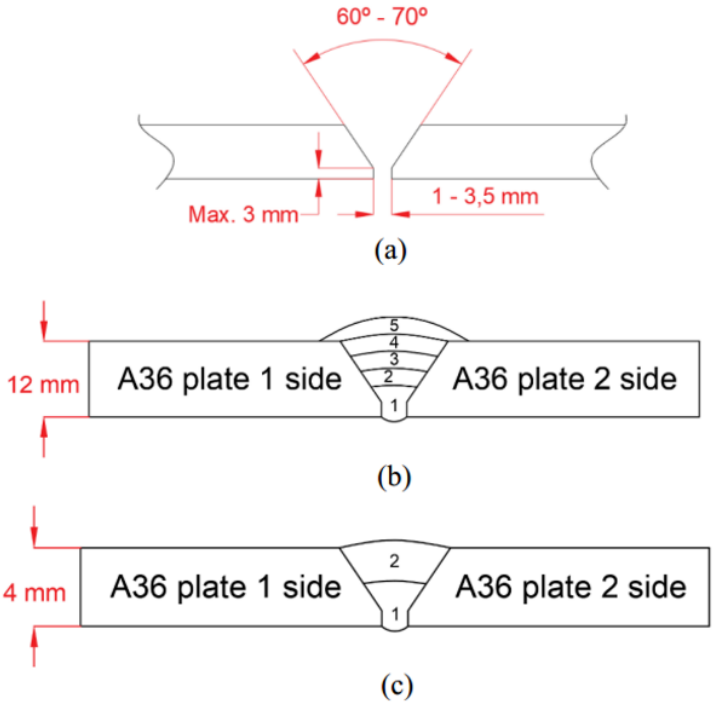

Figure 1. Schematic of welding process (a) Bevel design, (b) Five layers, and (c) Two layers

2.2. Welding Process and Parameters

Welding was performed using the SMAW process with rutile-coated electrodes (E6013, Ø3.2 mm). Two current levels, 70 and 80 A, were applied across the two plate thicknesses, resulting in four welded specimens. Welding was carried out in a flat position using bead-on-plate technique to ensure controlled and reproducible heat input. Table 1 explains the label based on the welding parameter.

Table 1. Welding parameter and label

Thickness of plate (mm)	Welding current (A)	Label
4	80	4A
4	70	4B
12	80	12A
12	70	12B

Konversi Energi dan Manufaktur
P-ISSN : 2339-2029
E-ISSN : 2622-5565
Jurnal Konversi Energi dan Manufaktur
Volume 11 Number 1 – January 2026 Page 1-8
Website : http://journal.unj.ac.id/unj/index.php/jkem
DOI: https://doi.org/10.21009/JKEM.11.1.1

2.3. Measurement of Temperature Distribution

The thermal distribution during welding was measured using K-type thermocouples attached at predefined distances (5, 10, and 15 mm) from the weld centerline on the plate surface. A total of 11 thermocouple measurement points (designated CH01 – CH11) were connected to a digital data logger operating at a sampling rate of 1 Hz. The recorded temperature profiles were used to analyze the effect of plate thickness and current variation on heat transfer and cooling rates.

2.4. Hardness Testing

Vickers hardness tests were performed in accordance with ASTM E384 [14]. Measurements were taken across the weld cross-section, covering the weld metal (WM), heat-affected zone (HAZ), and base metal (BM). A test load of 500 g was applied for 10 seconds, with an indentation spacing of 0.5 mm to avoid interference between impressions. Average hardness values were calculated for each zone.

2.5. Macrostructural Examination

Macrostructure evaluation was conducted to observe weld bead geometry, penetration depth, and fusion quality. Polished specimens were etched with 2% Nital and observed using an optical stereomicroscope. Weld continuity and defect formation were also recorded.

2.6. Microstructural Analysis

Metallographic samples were cut transverse to the weld bead. The samples were mounted, ground, and polished, then etched using 2% Nital solution to reveal microstructural features. Examination was performed using an optical microscope (OM) at magnifications of 200 to 500×. Microstructural phases such as ferrite, pearlite, widmanstätten ferrite, and acicular ferrite were identified.

3. Results and Discussion

3.1. Hardness Distribution

Figure 2 illustrates the hardness profiles of the welded specimens. In general, the highest hardness values were observed in the WM, followed by the BM, while the HAZ consistently exhibited the lowest values. This reduction in HAZ hardness is associated with grain coarsening and slower cooling rates. The maximum hardness recorded was 198.387 HVN for the 4 mm plate welded at 70 A (4B), attributable to its finer widmanstätten and acicular ferrite formation. Conversely, thicker plates welded at higher currents displayed lower hardness values, correlating with their ferrite-dominant microstructures.

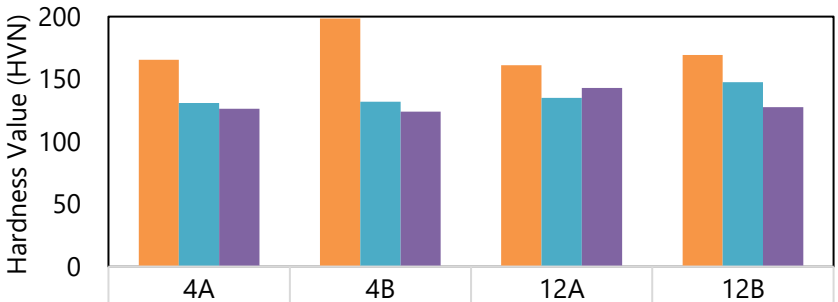

	4A	4B	12A	12B
WM	165.48	198.39	161.00	169.33
HAZ	130.82	131.97	135.00	147.62
BM	126.28	123.95	143.02	127.69

Figure 2. Hardness value comparison of welded A36 steel

Konversi Energi dan Manufaktur
P-ISSN : 2339-2029
E-ISSN : 2622-5565
Jurnal Konversi Energi dan Manufaktur
Volume 11 Number 1 – January 2026 Page 1-8
Website : http://journal.unj.ac.id/unj/index.php/jkem
DOI: https://doi.org/10.21009/JKEM.11.1.1

3.2. Temperature Distribution

The thermal profiles measured using thermocouples depicted in Figure 3 confirmed that plate thickness and welding current significantly affect heat flow and cooling rate. Thicker plate (12 mm) retained heat for longer periods, as indicated by the greater number of peak temperatures occurred within the specimen, and resulted in a slower cooling rate. Consequently, this produced a wider HAZ and coarser grains, and furthermore, it promoted the formation of more equilibrium phases such as ferrite and pearlite, thus, reducing the fraction of widmanstätten ferrite. On the other hand, the thinner plate (4 mm) promoted steeper cooling gradients, as heat dissipated rapidly into the surroundings; this is confirmed by the lower number of peak temperatures shown in Figure 3. As a result, this specimen exhibited a narrower HAZ and finer microstructural features with higher fraction of widmanstätten ferrite.

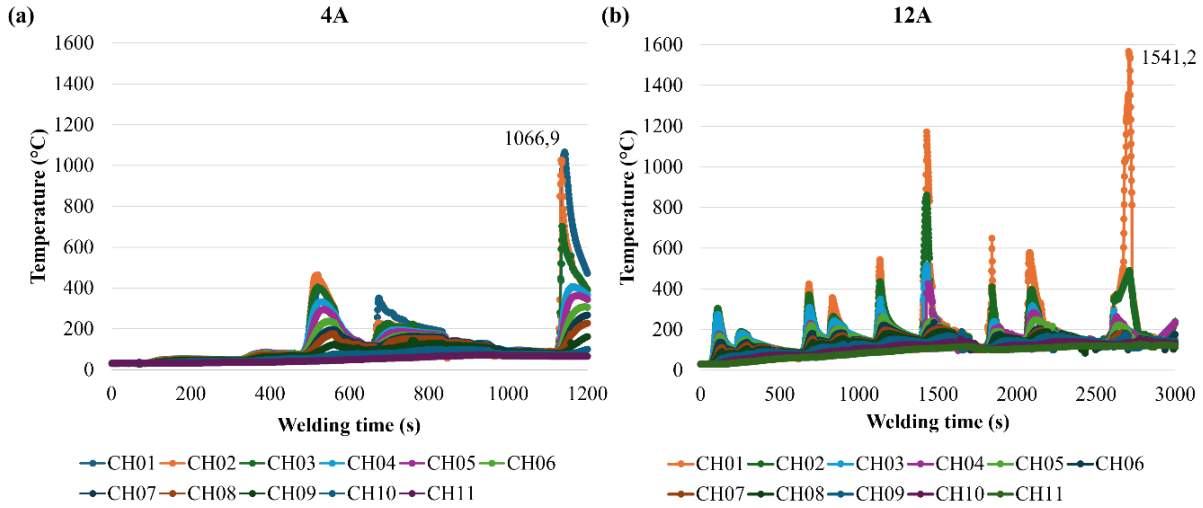

Figure 3. Temperature distribution of welded A36 steel (a) 4A and (b) 12A

3.3. Microstructural Distribution

The microstructural features of WM, HAZ, and BM varied significantly with welding parameters as seen in Figure 4.

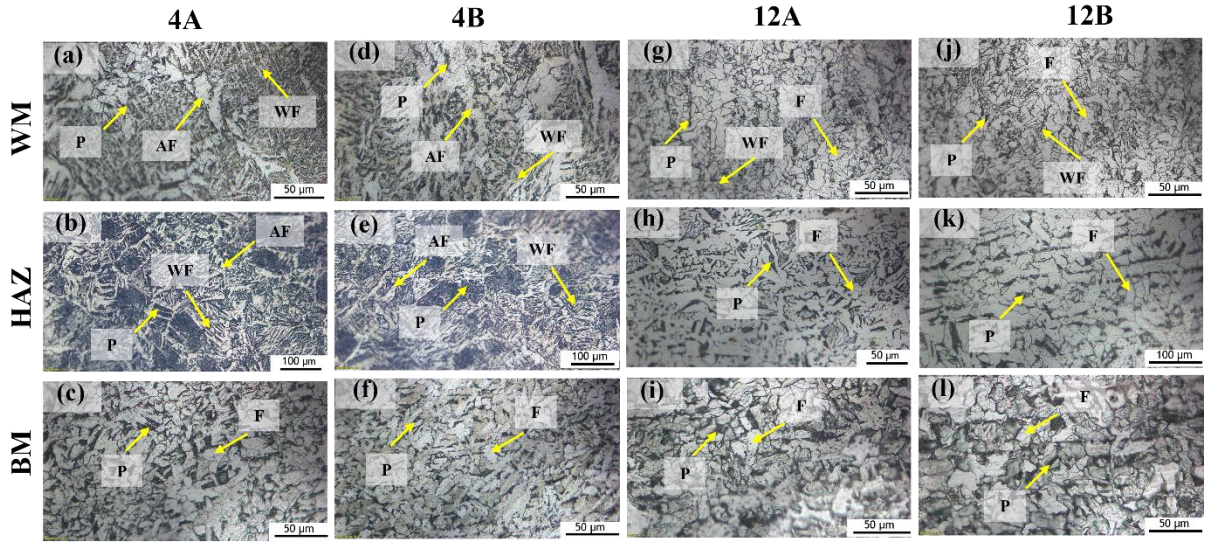

Figure 4. Microstructure result of welded A36 steel. F, P, AF, and WF are respectively ferrite, pearlite, acicular ferrite, and widsmantatten ferrite (a) WM 4A, (b) HAZ 4A, (c) BM 4A, (d) WM 4B, (e) HAZ 4B, (f) BM 4B, (g) WM 12A, (h) HAZ 12A, (i) BM 12A, (j) WM 12B, (k) HAZ 12B, and (l) BM 12B

Konversi Energi dan Manufaktur
P-ISSN : 2339-2029
E-ISSN : 2622-5565
Jurnal Konversi Energi dan Manufaktur
Volume 11 Number 1 – January 2026 Page 1-8
Website : http://journal.unj.ac.id/unj/index.php/jkem
DOI: https://doi.org/10.21009/JKEM.11.1.1

For 4 mm and 12 mm plates welded at 80 A (4A and 12A), the BM predominantly consisted of ferrite (bright phase) with pearlite (dark phase) as a secondary phase (Figures 4 (c) and (i)). The HAZ of 4A revealed widmanstätten ferrite with needle-like structure, acicular ferrite, and pearlite, while its WM contained a higher fraction of widmanstätten ferrite, indicating rapid cooling. In contrast, the 12A specimen exhibited a slower cooling rate, as reflected by its ferrite-dominant HAZ with only minor widmanstätten and acicular ferrite.

For specimens welded at 70 A (4B and 12B), the BM also consisted mainly of ferrite and pearlite (Figures 4 (i) and (l)). The HAZ of 4B showed widmanstätten ferrite, acicular ferrite, and pearlite, while the WM displayed an even greater amount of widmanstätten ferrite due to rapid cooling (Figure 4 (a)). In the 12B specimen, the slower cooling rate in thicker plates was evident, with ferrite–pearlite dominating the HAZ and a smaller portion of widmanstätten observed in the WM. These results demonstrate that both plate thickness and welding current strongly influence phase transformation and cooling behavior.

3.4. Macrostructural Analysis

Figure 5 presents the macrostructures of A36 welded specimens under different welding parameters. Overall, the joints were free from major defects such as porosity, undercut, or incomplete penetration, indicating proper process control. However, the specimen welded at 80 A with a 12 mm plate thickness (12A) exhibited slight angular distortion, consistent with higher heat input and slower cooling rate. Thicker plates and higher currents also produced a broader heat-affected zone (HAZ), whereas thinner plates welded at lower currents yielded narrower HAZ regions. This finding confirms with previous research that cooling rate plays a critical role in defining HAZ width [15].

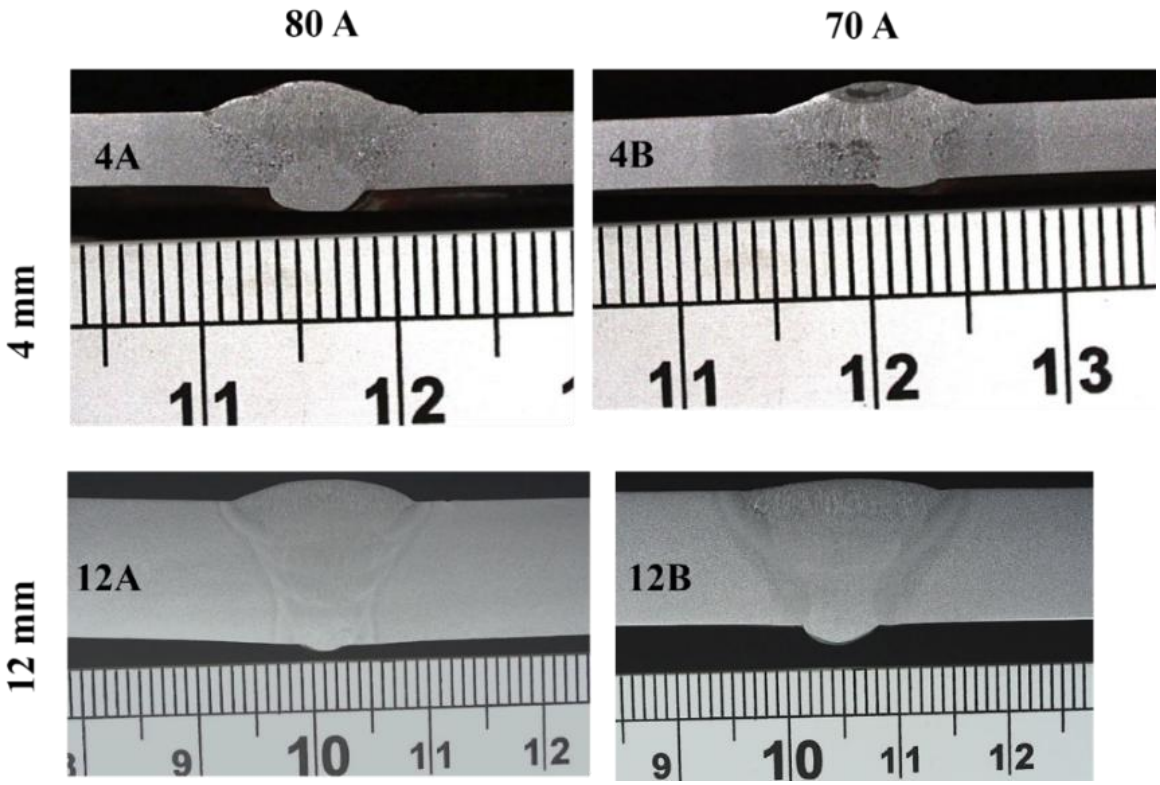

Figure 5. Macrostructure analysis of specimens. (Note: The marked part could form due to etching process. Non-uniform surface preparation caused the etchant to form etched grooves that look like defects and produced localized deep roughness).

Konversi Energi dan Manufaktur
P-ISSN : 2339-2029
E-ISSN : 2622-5565
Jurnal Konversi Energi dan Manufaktur
Volume 11 Number 1 – January 2026 Page 1-8
Website : http://journal.unj.ac.id/unj/index.php/jkem
DOI: https://doi.org/10.21009/JKEM.11.1.1

3.5. Discussion

The combined results indicate that welding current and plate thickness direct heat input and cooling behavior, thereby influencing hardness and microstructural evolution. An elevated welding current increases the heat input, hence raising the temperature within WM and the HAZ, as confirmed by the temperature distribution analysis. This elevation reduces the thermal gradient between these regions, resulting in a slower cooling rate in the WM of the 4A and 12A specimens [16], [17]. Consequently, only a small amount of widmanstätten formed in the WM, which corresponded to a lower hardness value; this result is in agreement with previous report [18]. On the other hand, a faster cooling rate occurred in the 4B and 12B specimens with lower welding current due to heat input decrease. Moreover, the thickness of the specimen significantly affects the cooling rate in the WM, with thicker plate exhibiting slower thermal dissipation. The thicker plates retain heat longer, resulting in slower cooling rates, which affects microstructure and mechanical properties of the weld zone [19], [20]. Lower current and thinner plates produce finer microstructures (acicular and widmanstätten ferrite) and higher hardness. However, higher current and thicker plates promote ferrite–pearlite formation with lower hardness.

These findings are consistent with prior studies on SMAW and other fusion welding processes [4], [13]. From an application perspective, selecting appropriate current and plate thickness combinations is essential to optimize weld quality and mechanical performance for LNG tank outer shells.

4. Conclusion

This study demonstrates that welding parameters, particularly plate thickness and welding current, play a decisive role in controlling hardness, thermal behavior, and the evolution of micro–macro structures in SMAW-welded ASTM A36 steel. Lower current (70 A) and thinner plates (4 mm) promoted steeper cooling gradients, resulting in the formation of finer microstructures such as widmanstätten and acicular ferrite and consequently higher hardness in the weld metal. In contrast, thicker plates (12 mm) and higher current (80 A) produced coarser ferritic structures, wider heat-affected zones, and reduced hardness due to slower cooling. The novelty of this work lies in integrating hardness testing, temperature distribution analysis, and comprehensive micro–macrostructural characterization to establish a direct correlation between welding parameters and weld quality in medium-thickness A36 steel, which has not been widely reported in previous studies.

From a practical perspective, these findings provide valuable input for optimizing welding procedures in the fabrication of ISO LNG tank shells, where minimizing heat input and promoting finer microstructures are critical for achieving reliable weld performance. Further research could expand this approach by incorporating advanced thermal modeling and extended mechanical testing, such as toughness and fatigue, to complement the present findings and enhance industrial application.

5. Acknowledgments

The authors would like to express their gratitude to Politeknik Perkapalan Negeri Surabaya for providing research facilities and technical support. This work was financially supported by Research Scheme B, DIPA 2025.

6. References

[1] T. Muttaqie, C. Sasmito, Iskendar, and A. Kadir, "Structural strength assessment of 20-ft LNG ISO tank: an investigation of finite element analysis and ASME design guidance," *IOP Conference Series: Earth and Environmental Science*, vol. 972, no. 1, p. 012015, 2022, doi: 10.1088/1755-1315/972/1/012015.

[2] F. Marpaung, E. T. Wibowo, and R. Harmadi, "Desain dan analisis tanki ISO LNG kapasitas 40 feet menggunakan teknik finite element analysis," *Jurnal Asiimetrik: Jurnal Ilmiah Rekayasa & Inovasi*, vol. 4, no.2, pp. 163–170, 2022, doi: 10.35814/asiimetrik.v4i1.2989.

[3] E. Turan, T. Kocal, and K. Ünlügençoğlu, "Welding technologies in shipbuilding industry," *Tojsat*, vol. 1, no. 4, pp. 24–30, 2011.

Konversi Energi dan Manufaktur
P-ISSN : 2339-2029
E-ISSN : 2622-5565
Jurnal Konversi Energi dan Manufaktur
Volume 11 Number 1 – January 2026 Page 1-8
Website : http://journal.unj.ac.id/unj/index.php/jkem DOI: https://doi.org/10.21009/JKEM.11.1.1

[4] W. L. Dhanistha, H. Pratikno, S. D. P. Maharani, Suntoyo, Silvianita, and D. Satrio, "Comparative analysis of welding mechanical properties FCAW welding joint of A36 and A53," *IOP Conference Series: Earth and Environmental Science*, vol. 1198, no. 1, p. 012035, 2023, doi: 10.1088/1755-1315/1198/1/012035.

[5] D.-Y. Lee, J.-S. Jo, A. J. Nyongesa, and W.-J. Lee, "Fatigue analysis of a 40 ft LNG ISO tank container," *Materials*, vol. 16, no. 1, p. 428, 2023, doi: 10.3390/ma16010428.

[6] S. Kou, "Welding metallurgy," 2nd ed. Hoboken, NJ, USA: John Wiley & Sons, 2003.

[7] K. Srinivasan, V. Balasubramanian, and M. Salahuddin, "Effect of heat input on emissions during shielded metal arc welding of mild steel," *Indian Welding Journal*, vol. 43, no.3, pp. 22–31, 2010.

[8] R. Nopriantoko, "Advancements in Welding technology: a review of techniques, materials, and applications," *Journal Applied Geo-mining and Metallurgy*, vol. 2, no. 1, pp. 62-110, 2025, doi: 10.1234/jm6e4w53.

[9] D. Deng, "Theoretical prediction of welding distortion in large and complex structures," *Frontiers of Materials Science in China*, vol. 4, no. 2, pp. 202-209, 2010, doi: 10.1007/s11706-010-0019-y.

[10] J. Sawicki, W. Stachurski, P. Kuryło, E. Tertel, B. Januszewicz, E. B-. Steinmetz, and A. Bednarek, "Comparative analysis of the dimensional accuracy and surface characteristics of gears manufactured using the 3D printing (DMLS) technique from 1.2709 steel," *Materials*, vol. 18, no. 7, p. 1461, 2025, doi: 10.3390/ma18071461.

[11] J. Anggono and R. Alimin, "Pengaruh besar input panas pengelasan SMAW terhadap distorsi angular sambungan t baja lunak ss400," *Jurnal Teknik Mesin*, vol. 1, no.1, pp. 45-54, 1999.

[12] R. H. Duan, G. M. Xie, P. Xue, Z. Y. Ma, Z. A. Luo, C. Wang, R. D. K. Misra, and G. D. Wang, "Microstructural refinement mechanism and its effect on toughness in the nugget zone of high-strength pipeline steel by friction stir welding," *Journal of Materials Science & Technology*, vol. 93, pp. 221–231, 2021, doi: 10.1016/j.jmst.2021.04.008.

[13] E. Ajenifuja, A. P. I. Popoola, and O. Popoola, "Comparative analysis of structural and mechanical properties of duplex stainless steel (DSS) weldments prepared by flux core arc welding and shielded metal arch welding processes," *Journal of Advanced Joining Processes*, vol. 11, p. 100295, 2025, doi: 10.1016/j.jajp.2025.100295.

[14] American Society for Testing and Materials, "Standard test method for microindentation hardness of materials," 2022.

[15] S. Yu. Maksymov, G. V. Fadeeva, J. Chuanbao, V. A. Kostin, A. A. Radzievskaya, and D. V. Vasilyev, "Influence of cooling rate on microstructure and phase composition of HAZ of duplex (DSS) 2205 steel in wet underwater welding," *The Paton Welding Journal*, vol. 2024, no. 1, pp. 3–12, 2024, doi: 10.37434/tpwj2024.01.01.

[16] A. I. S. and E. E., "Effect of arc welding current on the mechanical properties of A36 carbon steel weld joints," *SSRG International Journal of Mechanical Engineering*, vol. 2, no. 9, pp. 79–87, 2015, doi: 10.14445/23488360/ijme-v2i9p113.

[17] P. Kumar, A. N. Sinha, C. K. Hirwani, M. Murugan, A. Saravanan, and A. K. Singh, "Effect of welding current in TIG welding 304L steel on temperature distribution, microstructure and mechanical properties," *Journal of the Brazilian Society of Mechanical Sciences and Engineering*, vol. 43, no. 369, 2021, doi: 10.1007/s40430-021-03082-6.

[18] S. Senthilkumar, S. Manivannan, R. Venkatesh, and M. Karthikeyan, "Influence of heat input on the mechanical characteristics, corrosion and microstructure of ASTM A36 steel welded by GTAW technique," *Heliyon*, vol. 9, no. 9, 2023, doi: 10.1016/j.heliyon.2023.e19708.

[19] A. de A. Vicente, R. L. de Souza, D. C. R. Espinosa, R. R. de Aguiar, P. Paul, and A. B. B. Junior, "Effect of relative plate thickness in the heat flow and cooling rate during welding of super duplex stainless

Konversi Energi dan Manufaktur
P-ISSN : 2339-2029
E-ISSN : 2622-5565
Jurnal Konversi Energi dan Manufaktur
Volume 11 Number 1 – January 2026 Page 1-8
Website : http://journal.unj.ac.id/unj/index.php/jkem
DOI: https://doi.org/10.21009/JKEM.11.1.1

steel," *Saudi Journal of Engineering and Technology*, vol. 5, no. 5, pp. 244–250, 2020, doi: 10.36348/sjet.2020.v05i05.005.

[20] H-. H. Jo, K-. W. Kim, H. Park, J. Moon, Y-. W. Kim, H-. B. Shim, and C-. H. Lee, "Estimation of cooling rate of high-strength thick plate steel during water quenching," *Materials.*, vol. 16, no. 13, p. 4792, 2023, doi: 10.3390/ma16134792.